HEM1 deficiency disrupts mTORC2 and F-actin control in inherited immunodysregulatory disease

Sarah A. Cook[1]*, William A. Comrie[1,2]*, M. Cecilia Poli[3,4,5], Morgan Similuk[6], Andrew J. Oler[7], Aiman J. Faruqi[1], Douglas B. Kuhns[8], Sheng Yang[9], Alexander Vargas-Hernández[3,4], Alexandre F. Carisey[3,4], Benjamin Fournier[10,11], D. Eric Anderson[12], Susan Price[13], Margery Smelkinson[14], Wadih Abou Chahla[15], Lisa R. Forbes[3,4], Emily M. Mace[16], Tram N. Cao[3,4], Zeynep H. Coban-Akdemir[17,18], Shalini N. Jhangiani[18,19], Donna M. Muzny[18,19], Richard A. Gibbs[17,18,19], James R. Lupski[17,18,19], Jordan S. Orange[16], Geoffrey D. E. Cuvelier[20], Moza Al Hassani[21], Nawal Al Kaabi[21], Zain Al Yafei[21], Soma Jyonouchi[22,23], Nikita Raje[24,25], Jason W. Caldwell[26], Yanping Huang[27,28], Janis K. Burkhardt[27], Sylvain Latour[10,11], Baoyu Chen[9], Gehad ElGhazali[21], V. Koneti Rao[13], Ivan K. Chinn[3,4], Michael J. Lenardo[1]†

Immunodeficiency often coincides with hyperactive immune disorders such as autoimmunity, lymphoproliferation, or atopy, but this coincidence is rarely understood on a molecular level. We describe five patients from four families with immunodeficiency coupled with atopy, lymphoproliferation, and cytokine overproduction harboring mutations in *NCKAP1L*, which encodes the hematopoietic-specific HEM1 protein. These mutations cause the loss of the HEM1 protein and the WAVE regulatory complex (WRC) or disrupt binding to the WRC regulator, Arf1, thereby impairing actin polymerization, synapse formation, and immune cell migration. Diminished cortical actin networks caused by WRC loss led to uncontrolled cytokine release and immune hyperresponsiveness. HEM1 loss also blocked mechanistic target of rapamycin complex 2 (mTORC2)–dependent AKT phosphorylation, T cell proliferation, and selected effector functions, leading to immunodeficiency. Thus, the evolutionarily conserved HEM1 protein simultaneously regulates filamentous actin (F-actin) and mTORC2 signaling to achieve equipoise in immune responses.

Inborn errors of immunity (IEIs) can affect global cellular regulatory systems (*1*). The mechanistic target of rapamycin complex 1 (mTORC1) and mTORC2 are global regulators of metabolism and cell signaling. mTORC2, comprising the mTOR, RICTOR, mSIN1, mLST8, PROTOR1 and PROTOR2 (PROTOR1/2), and DEPTOR proteins, activates AGC kinases downstream of phosphoinositide 3-kinase (PI3K) to promote T cell survival, proliferation, and differentiation (*2–5*). Similarly, actin is a global regulator of cellular behavior and immune synapse (IS) formation (*6*, *7*). Signals activating the WAVE regulatory complex (WRC), which contains CYFIP1/2, HEM1/2, ABI1/2/3, HSPC300, and WAVE1/2/3, control the dynamics of Arp2/3-mediated branched filamentous actin (F-actin) nucleation and polymerization. In the WRC, HEM1/2 and CYFIP1/2 form a membrane-associated scaffold supporting the ABI1/2, HSPC300, and WAVE1/2/3 proteins and are directly activated by the small guanosine triphosphatases (GTPases) Rac1 and Arf1, although the Arf1 binding site is uncertain (*8*, *9*) (Fig. 1). Whether the WRC regulates the cortical actin network (CAcN) is unknown (*6–12*). Mutations affecting actin regulatory proteins underlie immunodeficiencies (table S1), but none have been reported yet for WRC components (*13*).

We investigated five patients from four unrelated families with recurrent bacterial and viral skin infections, severe respiratory tract infections leading to pneumonia and bronchiectasis (Fig. 1, A and B, left panels, and fig. S1A), and poor specific antibody responses (Fig. 1B, right panel, and table S2). Paradoxically, these patients also exhibited atopic and inflammatory disease alongside chronic hepatosplenomegaly and lymphadenopathy, sometimes with elevated immunoglobulin E (IgE) or IgG and autoimmune manifestations (Fig. 1B; fig. S1, B and C; and tables S2 and S3). FoxP3^{+} T regulatory cells were normal (fig. S1D). All five patients harbored biallelic *NCKAP1L* mutations encoding missense variants in HEM1, the hematopoietic-specific member of the WRC (Fig. 1, A and C, and table S4). The amino acid substitutions affected conserved residues that were not homozygous in the Genome Aggregation Database (gnomAD) or internal databases and were bioinformatically predicted to be damaging (fig. S2, A and B) (*14*). The altered residues clustered within the quaternary structure of the WRC near the distal Rac1-binding site located on CYFIP1/2 (fig. S2, A to D), which we call the HEM1 regulatory site (HRS). The human immune phenotype differs from the lymphopenia, neutrophilia, or bone marrow failure observed in HEM1-deficient mice (*12*, *15*, *16*).

Biochemical analyses showed that patients 1.1, 2.1, 2.2, and 4.1 lost HEM1, CYFIP1, and WAVE2, which indicates WRC destabilization, whereas patient 3.1 expressed normal levels of WRC proteins (Fig. 1D and fig. S3, A to C). Moreover, the HEM1 substitutions in patients 1.1 and 2.1, but not in patient 3.1, reduced affinity for WAVE2 (Fig. 1E and fig. S3D). The WRC could be restored in *NCKAP1L* CRISPR-Cas9 knockout (HEM1-KO) Jurkat cells by wild-type and patient 3.1 HEM1 but less so by the patient 1.1 and 2.1 variants (fig. S3E). Immunoprecipitation–mass spectrometry (IP-MS) showed that the Met[371]→Val (M371V) HEM1 variant (patient 3.1) maintained association with HEM1- and WAVE2-interacting proteins (fig. S4 and table S5). We therefore hypothesized that M371V disrupted the activation by either Rac1 or Arf1, the small GTPases that activate the WRC. By reconstituting the WRC in vitro with recombinant proteins (containing HEM2 with the equivalent M373V substitution, but not HEM1, which had an insufficient yield), we observed that the HEM2-M373V protein interacted poorly with GST-Arf1 and could not promote F-actin polymerization upon stimulation with an Arf1-Rac1 dimer (Fig. 1F and fig. S3, F to H). Thus, the Met[371/373] residues

located in the HRS of HEM1/2 are crucial for Arf1 binding and WRC activation, which is analogous to binding of Rac1 to CYFIP1/2 (8). Therefore, the patient HEM1 mutants either destabilize the WRC or disrupt its Arf1-mediated activation (fig. S2E).

We observed that interleukin-2 (IL-2) stimulation caused patient and HEM1-knockdown cells to hypersecrete perforin and granzymes and hyperproliferate in response to IL-2 (Fig. 2, A and B, and fig. S5, A, B, and E). Proximal IL-2 signaling was normal, which implies that downstream processes, such as CAcN control of granule release, might have been affected (fig. S6) (17–19). We found evidence for an abnormal CAcN because patient cells displayed reduced cortical F-actin and aberrant mem-

brane spikes and puncta caused by unregulated formin and WASp, respectively (Fig. 2C and movie S1) (20). We also observed defective cell spreading and lamellipodia (fig. S5C). Patient T cells expressed higher levels of surface CD107a (LAMP1), which indicates increased granule membrane fusion, especially after phorbol myristate acetate and ionomycin–induced degranulation (Fig. 2D and fig. S5D). Experimental reduction of HEM1 in primary T cells and NKL cells also increased the release of cytokines and granule contents, CD107a expression, or both (fig. S5, E to H). Three-dimensional imaging revealed a diminished CAcN and a notable accumulation of lytic granules at the IS of patient cells (Fig. 2E). Latrunculin A (LatA), which depolymerizes

F-actin, increased exocytosis-based CD107a surface expression and the release of granzymes A and B in a dose-dependent manner (Fig. 2D, bottom, and fig. S5, I and J). Thus, the WRC containing HEM1 enables the CAcN to restrain excessive degranulation and granule release by T cells. Constitutive cytokine release was blocked by a Jak inhibitor (fig. S5E).

We next explored other F-actin functions using live-cell imaging of the T cell IS and found that patient cells and HEM1-KO Jurkat cells reconstituted with mutant HEM1 alleles cannot form symmetrical and stable synaptic contacts with the coverslip (movies S1 and S2) (20). We also observed abnormal formin spikes, WASp-mediated puncta, and defective lamellipodia. Because lamellipodia guide cell migration,
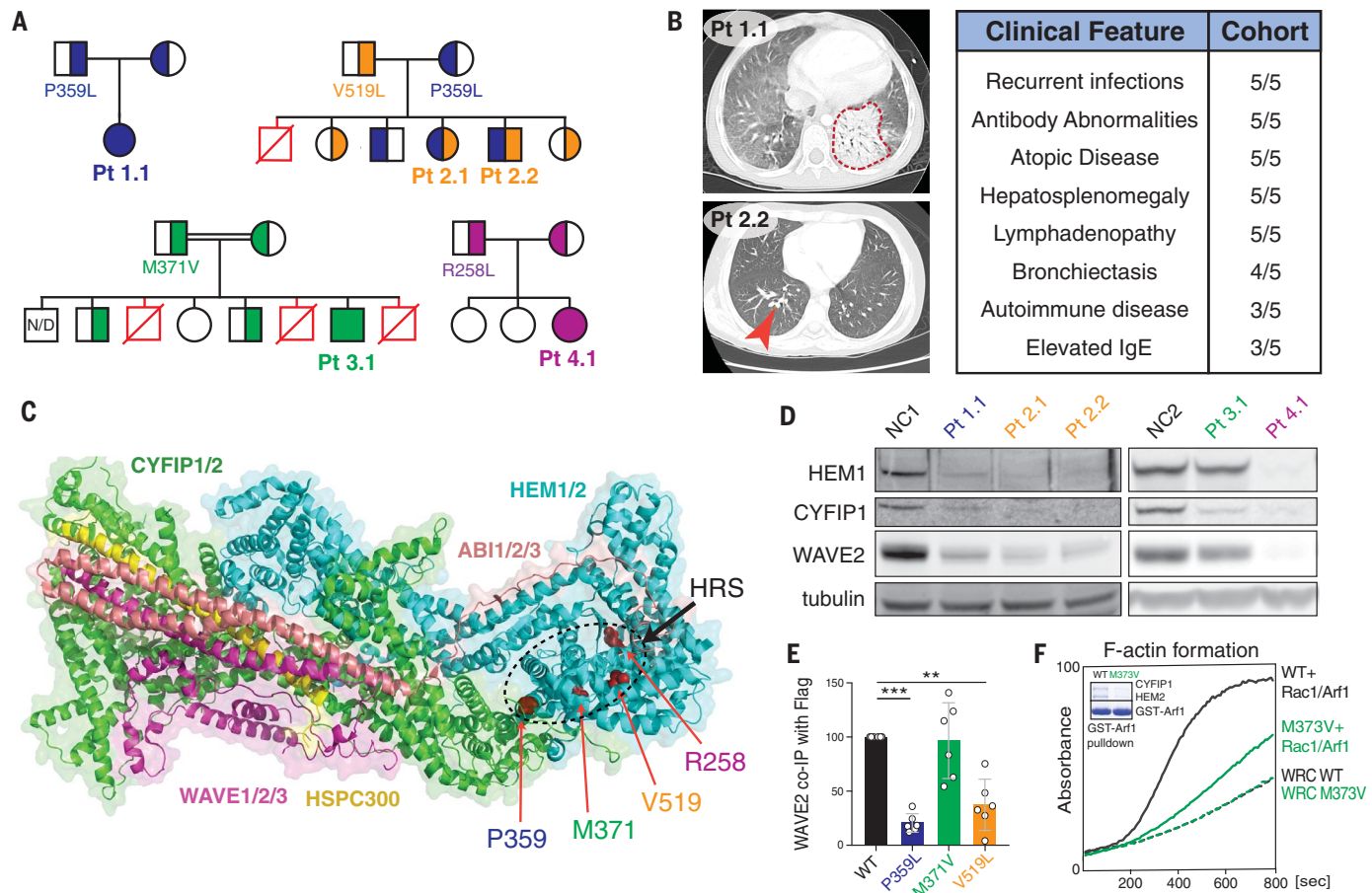
Fig. 1. Immunodysregulatory disorder caused by genetic HEM1 deficiency. (**A**) Patient (Pt) pedigrees showing recessive inheritance of disease and HEM1 amino acid substitutions. Red symbols indicate deceased affected siblings of unknown genotype. N/D, not determined. (**B**) Chest computed tomography (CT) scans showing ground glass opacity and pneumonia (red outline) in Pt 1.1 (upper left) and bronchiectasis (red arrow) in Pt 2.2 (bottom left). Key shared clinical features are also noted (right). (**C**) Structural location of patient variants in HEM1 in the WRC (Protein Data Bank: 3P8C; PubMed ID: 21107423). HRS, HEM1 regulatory site. (**D**) Immunoblot of WRC components in lysates derived from Pt and normal control (NC) CD4⁺ (left) and CD8⁺ (right) T cell blasts. (**E**) Quantification of WAVE2

coimmunoprecipitated (co-IP) by wild-type (WT) or mutant HEM1-Flag constructs in six independent experiments. Statistical analysis was performed using a one-sample t test. (**F**) Pyrene-actin polymerization assay with WRC230VCA containing HEM2 WT or M373V, with or without activation by a Rac1-Arf1 heterodimer preloaded with GMPPNP. (Inset) Coomassie blue–stained gel showing GST-Arf1 pull-down of WRC230VCA containing HEM2 WT or M373V and Rac1 (Q61L/P29S). Data are representative of four independent experiments. **$P \leq 0.01$; ***$P \leq 0.001$. Single-letter abbreviations for the amino acid residues are as follows: A, Ala; C, Cys; D, Asp; E, Glu; F, Phe; G, Gly; H, His; I, Ile; K, Lys; L, Leu; M, Met; N, Asn; P, Pro; Q, Gln; R, Arg; S, Ser; T, Thr; V, Val; W, Trp; and Y, Tyr.
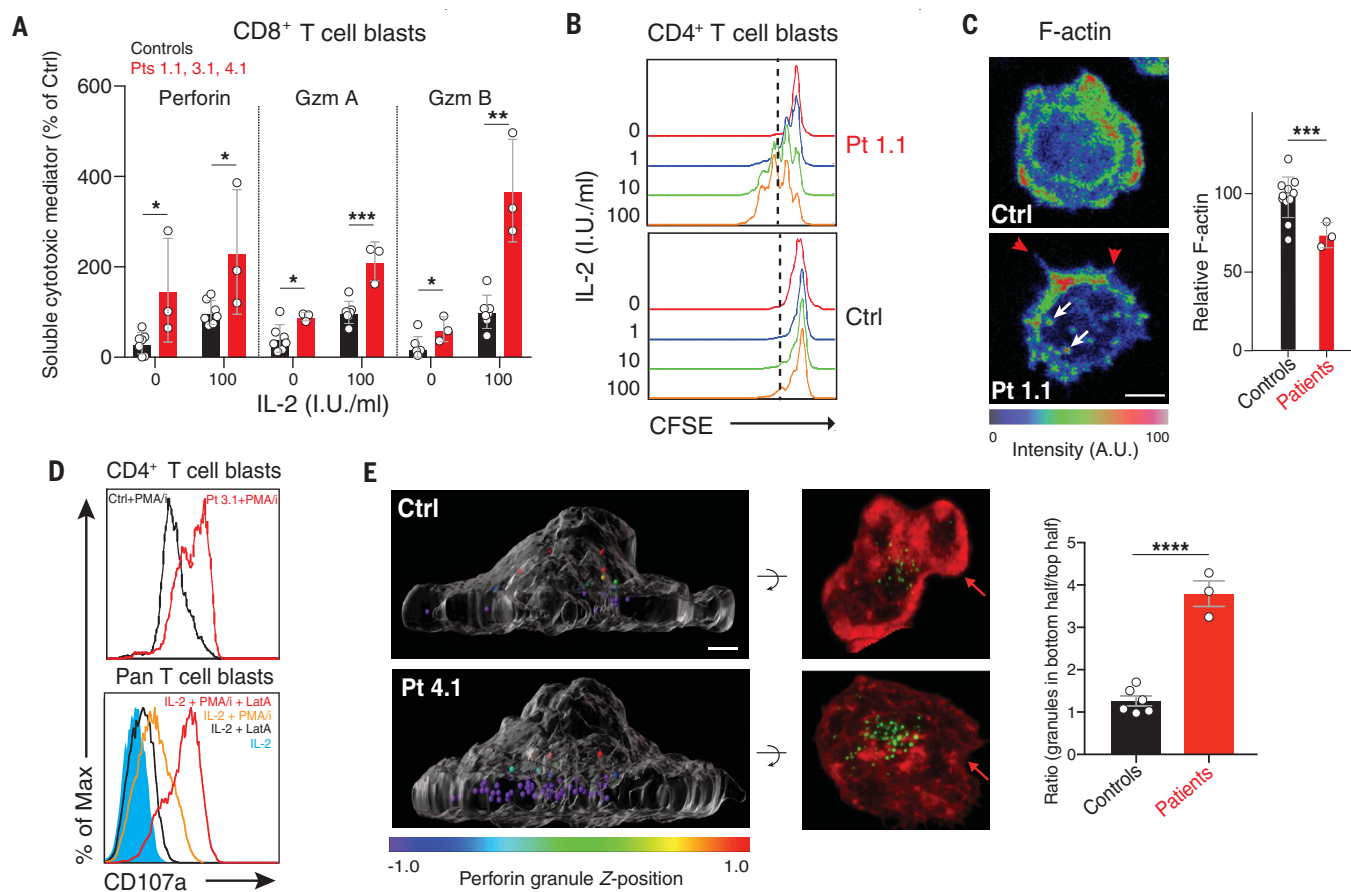
Fig. 2. HEM1 is essential for regulating cortical actin and granule release.
(**A**) Release of granzymes (Gzm) A and B or perforin from Pt or control (Ctrl) CD8^{+} T cell blasts after 18 hours of IL-2 stimulation in international units (I.U.) in three independent experiments. (**B**) Flow cytometric histograms measuring proliferation of rested CD4^{+} T cell blasts from a normal control (Ctrl) or patient 1.1 (Pt 1.1) measured by carboxyfluorescein succinimidyl ester (CFSE) dilution after IL-2 restimulation for 96 hours. (**C**) (Left) Ctrl or Pt 1.1 CD4^{+} T cell blasts spreading on coverslips coated with anti-CD3, anti-CD28, and ICAM-1 (1 μg/ml each), stained with phalloidin, and pseudocolored for F-actin. (Right) F-actin was quantified in three experiments. Red arrows indicate formin-mediated spikes, and white arrows indicate WASp-mediated actin puncta. Scale bar, 4 μm.

(**D**) Surface CD107a on Ctrl and Pt 3.1 CD4^{+} T cell blasts after 1 hour of phorbol myristate acetate (PMA)/ionomycin (I) stimulation (top) or stimulated pan T cells with 1 μM latrunculin A (LatA) (bottom). (**E**) (Left) Side view of perforin granules pseudocolored by Z-position relative to the cell center in Ctrl or Pt 1.1 CD8^{+} T cell blasts. (Middle) Corresponding 90° forward rotation top views of F-actin (red) and perforin (green). Red arrows indicate lamellipodial F-actin density. Scale bar, 2 μm. (Right) Mean ratios of granules in the bottom half to top half of the cell, quantified in at least 30 cells per sample. Bars represent means ± SEM (control, $n = 6$; patient, $n = 3$). Data represent at least three repeat experiments. Statistical analyses for (A), (C), and (E) were performed using a t test without assuming equal variance. *$P \leq 0.05$; **$P \leq 0.01$; ***$P \leq 0.001$; ****$P \leq 0.0001$.

we evaluated spontaneous T cell and neutrophil migration (*21, 22*). We found that patient T cells exhibited defective membrane ruffling; loss of lamellipodial extensions; decreased F-actin density at the leading edge with abnormal puncta, spikes, and blebs; and reduced migratory velocity (fig. S7, A and B, and movie S3). Similarly, patient neutrophils migrating in chemokine gradients exhibited reduced velocity and directional persistence, unusual elongation, and misdirected competing leading edges (Fig. 3, A and B; movie S4; and fig. S7C). In patients for whom we had sufficient samples, we found decreased natural killer (NK) cell abundance along with defective F-actin accumulation at the IS and a corresponding defect in conjugate formation (Fig. 3, C and D, and fig. S7E). Additionally, HEM1-KO NKL clones dis-

played reduced effector function after stimulation (fig. S7, F and G).

We also found abnormal T cell activation manifested by reduced CD69 and CD25 expression, blunted proliferation, and decreased IL-2 and tumor necrosis factor (TNF) production (Fig. 3, E to G, and fig. S9, A and B). Additionally, patient T cells had defective integrin activation with lower soluble ICAM-1 binding, though adherence to immobilized ICAM-1 was largely intact, which indicates a defect in integrin affinity maturation. Notably, we found that CD8^{+} T cell cytotoxicity and the release of granzyme A, granzyme B, and perforin were normal (fig. S8, A to C, and fig. S9, C and D) (*21, 23, 24*). Proliferation and cytokine defects were recapitulated by short hairpin RNA (shRNA) knockdown of HEM1 (Fig. 3, H and I).

Despite the IS abnormalities, proximal T cell receptor (TCR) signaling events in HEM1-deficient patient cells were normal (fig. S10, A to C) (*21*). Nevertheless, we found that both patient and HEM1-knockdown T cells showed defective TCR-induced phosphorylation of a well-known substrate of the mTORC2 complex, AKT (protein kinase B), at Ser[473] (Fig. 4A and fig. S11, A to C) (*25*). Phosphorylation of mTORC2-independent targets, including AKT Thr[308] and ribosomal protein S6 Ser[235/236] and Ser[240/244], was moderately reduced in patient cells, but these defects were not recapitulated by HEM1 knockdown (Fig. 4B and fig. S11, C and D). Immunoblotting showed decreased phosphorylation of AKT Ser[473] as well as decreased Ser[21] of the downstream AKT substrate, glycogen synthase kinase (GSK) 3a
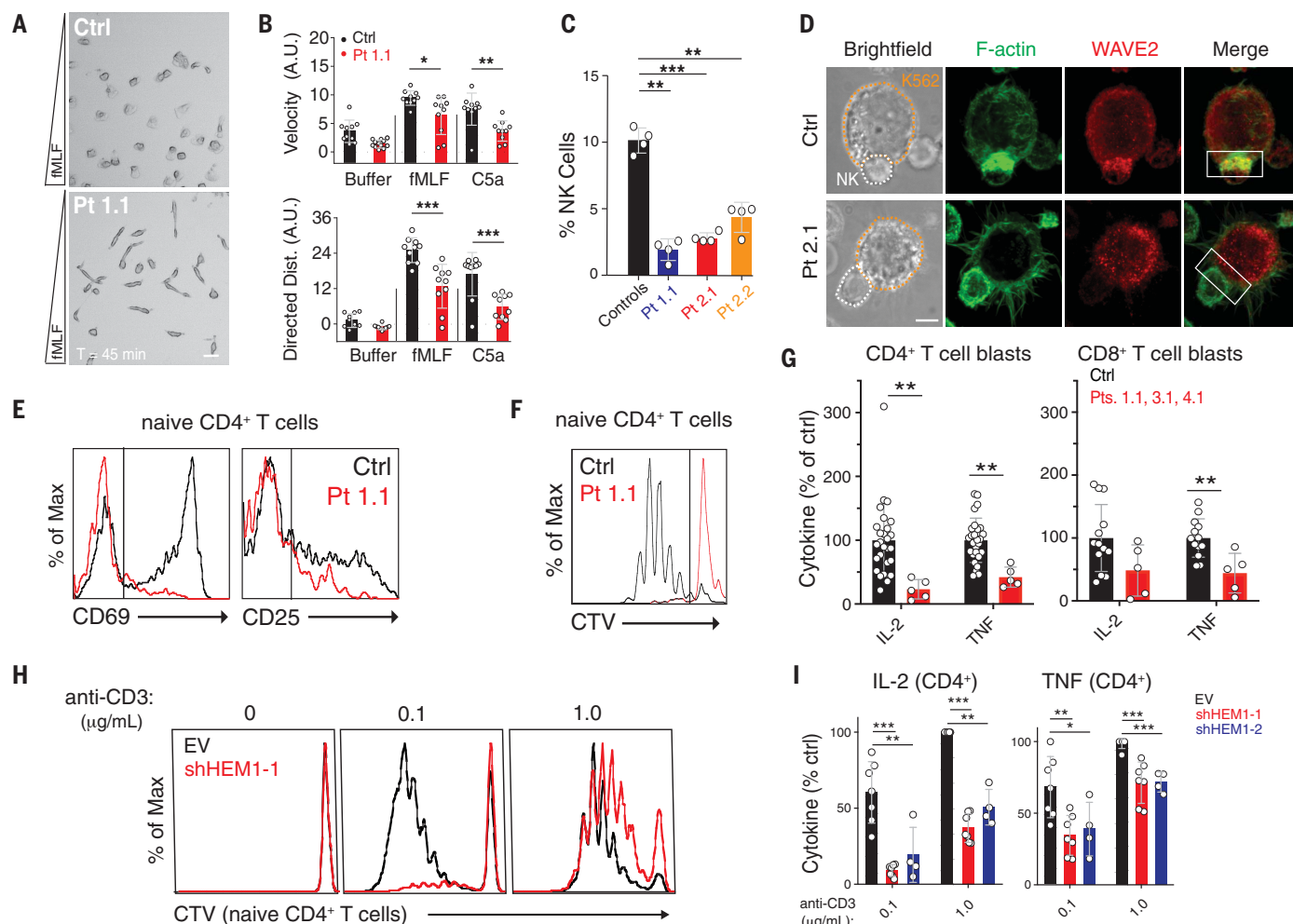
Fig. 3. HEM1 loss causes immunodeficiency by abnormal immune cell behavior and activation. (**A**) Single frame from movie S4 showing healthy Ctrl or Pt 1.1 neutrophils migrating in a gradient (bottom has the greatest concentration) of N-formyl-L-methionyl-L-leucyl-L-phenylalanine (fMLF). Scale bar, 20 μm. (**B**) Displacement velocity (top) and net directed distance (Dist.) (bottom) in arbitrary units (A.U.) of 10 randomly selected Ctrl or Pt 1.1 neutrophils migrating in chemoattractant gradients. (**C**) Percentage of NK cells in four peripheral blood samples. (**D**) Photomicrographs of immunological synapses between K562 target cells (orange outline) and NK cells (white outline) stained with phalloidin for F-actin and WAVE2 antibody. White boxes indicate area of synapse. Scale bar, 5 μm. (**E**) CD69 and CD25 up-regulation on Ctrl or Pt 1.1 naïve CD4+ T cells after stimulation with immobilized anti-CD3/28 (1 μg/ml each). Max, maximum. (**F**) Cell trace violet (CTV) proliferation plots of cells as in (E), stimulated for 5 days. (**G**) IL-2 and TNF secretion by CD4+ or CD8+ T cell blasts after restimulation for 36 hours with immobilized anti-CD3/28 and ICAM-1 (1 μg/ml each) in three independent experiments. (**H**) CTV plots of naïve CD4+ T cells transduced with empty vector (EV) or small hairpin RNA against HEM1 (sh-HEM1), stimulated on immobilized ICAM-1/anti-CD28 (1 μg/ml each) and the indicated dose of anti-CD3. (**I**) IL-2 and TNF secretion by CD4+ T cell blasts transduced with EV, sh-HEM1-1, or sh-HEM1-2 and stimulated as in (H). Neutrophil migration was analyzed for two independent donors; otherwise, data represent at least four independent trials of each assay. Statistical analyses for (B), (C), and (G) were performed using a *t* test without assuming equal variance. Statistical analysis for (I) was performed using a Wilcoxon matched-pairs signed-rank test. *$P \leq 0.05$; **$P \leq 0.01$; ***$P \leq 0.001$.

(Fig. 4C). TCR-induced AKT Ser[473] in T cells could be blocked by an mTOR catalytic inhibitor (Ku0063794), whereas inhibition of the actin network by LatA moderately enhanced AKT Ser[473] phosphorylation. Thus, the AKT Ser[473] phosphorylation defect appears to be independent of HEM1 regulation of the CaCN (fig. S11, E and F).

To investigate how HEM1 regulates the phosphoinositide 3-kinase (PI3K)–AKT–mTORC2 pathway, we searched our IP-MS datasets and found that several mTORC2 components—

including mTOR and RICTOR, the key scaffolding protein of mTORC2—were precipitated by HEM1 but not WAVE2 (fig. S4, fig. S12A, and table S5). This observation suggested the existence of a pool of HEM1 outside of the WRC that interacts with and regulates mTORC2 (*22*). Testing HEM1-Flag (wild-type, P359L, and M371V), Flag–green fluorescent protein (GFP), myc-RICTOR, or WAVE2 from 293T cells, we observed that HEM1, but not WAVE2, specifically coimmunoprecipitated with RICTOR (Fig. 4D and fig. S12, A and B). Notably, the

P359L HEM1 is strongly associated with RICTOR, which suggests that the interaction occurs when HEM1 is not in complex with the WRC. Knockdown of RICTOR in CD4+ T cells impaired proliferation and cytokine secretion (Fig. 4, E and F, and fig. S12D). Chemical inhibitors of the PI3K, AKT, or mTOR kinases also abrogated T cell proliferation and IL-2 and TNF secretion (fig. S12, E and F). Notably, specific inhibition of mTORC1 with rapamycin had little effect compared with inhibition of both complexes with an mTOR catalytic

inhibitor, which suggests that mTORC2, but not mTORC1, is required. However, mTOR inhibition had little effect on the secretion of perforin and granzymes or on CD69 and CD25 up-regulation, essentially phenocopying the defects observed in patient cells (fig. S12, G to I). Thus, HEM1 plays an additional role in human T cells outside of the WRC as an upstream regulator of mTORC2 enzymatic activity (Fig. 4G).

Previous studies have shown that individual WRC components can have noncanonical roles in cellular processes beyond actin filament nucleation and that HEM1/2 exists, and likely functions, outside of the WRC complex (11, 22). We now show that in human patients with immunodeficiency and immune hyperactivation, the loss-of-function mutations in *NCKAP1L*, the gene encoding HEM1, disrupt WRC-mediated actin polymerization and abrogate mTORC2 activation of AKT. The resulting autosomal
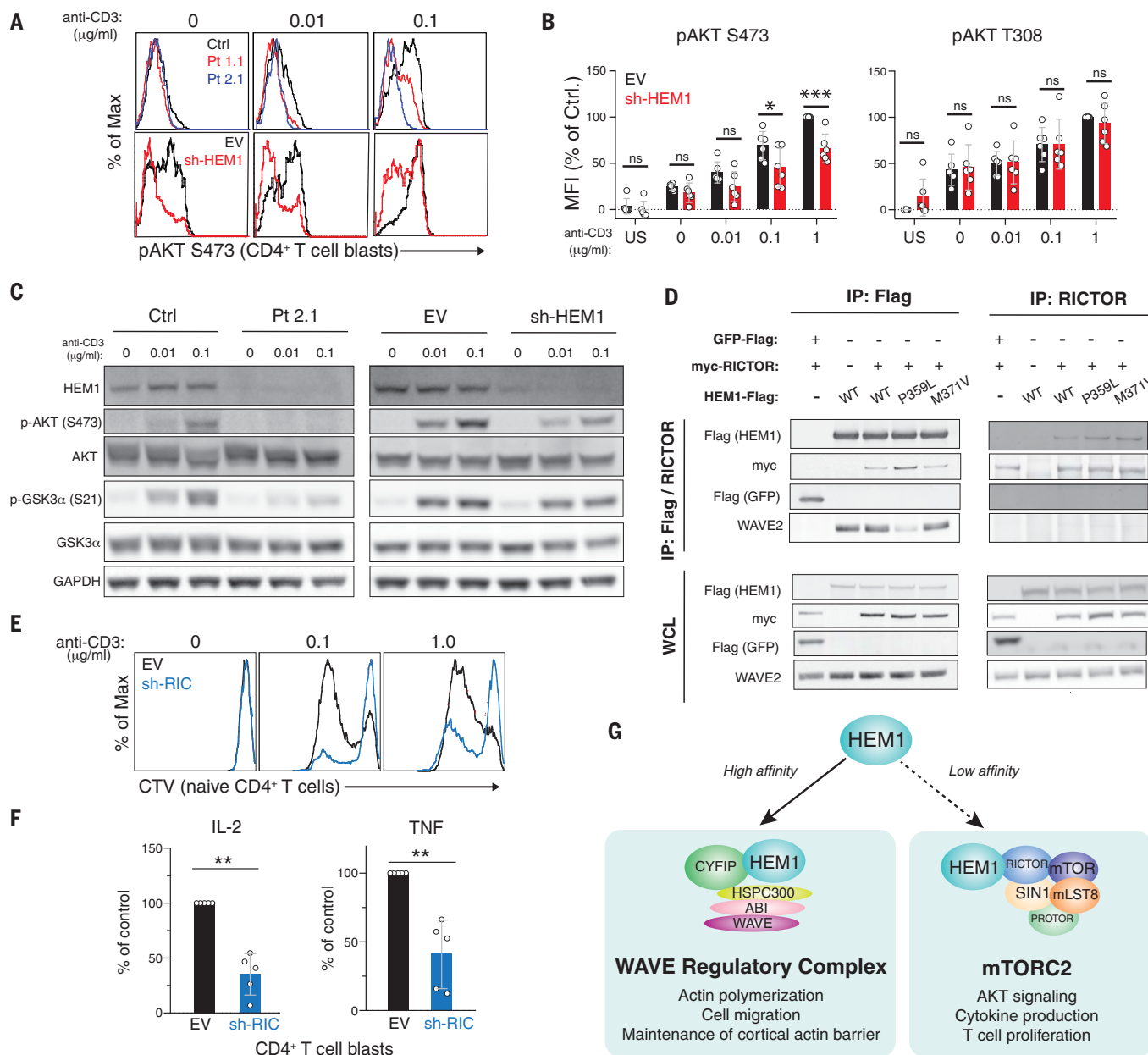
Fig. 4. HEM1 associates with RICTOR and governs mTORC2 activation.
(**A**) Phospho-flow cytometry of purified CD4⁺ T cell blasts from Ctrl or Pt (top row) or EV transduced or sh-HEM1 knockdown cells (bottom row) for AKT phosphorylated on Ser⁴⁷³ (pAKT S473). Cells were stimulated for 10 min with anti-CD28 and ICOS (1 μg/ml each) and the indicated dose of anti-CD3. (**B**) Mean fluorescence intensity (MFI) of pAKT S473 or AKT pAKT T308 in EV or sh-HEM1 CD4⁺ T cell blasts stimulated as in (A) in six independent experiments. US, unstimulated; ns, not significant. (**C**) Immunoblot of Ctrl or Pt CD4⁺ T cell blasts, or healthy CD4⁺ T cell blasts cells transduced with EV or sh-HEM1. Cells were rested and restimulated with ICAM-1 and anti-CD28 (1 μg/ml each) and the indicated dose of anti-CD3. (**D**) Flag and RICTOR IP from 293T cells transduced with myc-RICTOR and either Flag-tagged GFP or Flag-tagged HEM1 (WT or mutant) and blotted. (**E**) CTV proliferation plots of naïve CD4⁺ T cells transduced with EV or shRNA directed against RICTOR (sh-RIC). (**F**) Cytokine secretion by control and RICTOR knockdown (sh-RIC) CD4⁺ T cell blasts after 18-hour restimulation in five independent experiments. (**G**) Provisional model of HEM1 independently regulating WRC- and mTORC2-mediated functions. Statistical analyses for (B) and (F) were performed using a Wilcoxon matched-pairs signed-rank test. *P ≤ 0.05; **P ≤ 0.01; ***P ≤ 0.001.

recessive IEI affects multiple hematopoietic lineages and leads to bacterial and viral infections, atopic disease, autoimmunity, cytokine overproduction, and lymphoproliferative disease. We demonstrate that HEM1 and the WRC maintain the CAcN, which restricts cytokine secretion and lytic granule release. We also show that HEM1 plays a key binding role in Arf1-mediated WRC activation. Our findings suggest a broader effect of genetic HEM1 deficiency on the cytokine repertoire and cellular effector function that should be addressed in future work. Finally, we identify an interaction between HEM1 and RICTOR that is essential for mTORC2 regulation. HEM1 may have escaped detection in previous RICTOR precipitation experiments because the interaction appears to be weak and because commonly used 293T cells do not express the hematopoietically restricted HEM1. We posit that HEM1 independently coordinates WRC-mediated actin nucleation and mTORC2 catalytic activity in response to signals that activate both protein complexes—such as PI3K, Arf1, and Rac1—during T cell activation and possibly during B and NK cell activation. These data could explain how mTORC2 is activated downstream of actin-generated membrane tension and can negatively regulate the WRC (*26*). Because mTORC2 exerts similar roles in all lymphocytes, and because their activation involves actin-dependent regulation, it is likely that B and NK cell abnormalities contribute to immunopathology in the HEM1-deficient patients (*27–29*). Our study elucidates a human congenital disorder caused by loss of HEM1 and highlights potential routes for immunological therapy.

REFERENCES AND NOTES

1. C. Cunningham-Rundles, P. P. Ponda, *Nat. Rev. Immunol.* **5**, 880–892 (2005).
2. R. A. Saxton, D. M. Sabatini, *Cell* **169**, 361–371 (2017).
3. D. A. Guertin *et al.*, *Dev. Cell* **11**, 859–871 (2006).
4. K. Lee *et al.*, *Immunity* **32**, 743–753 (2010).
5. L. A. Van de Velde, P. J. Murray, *J. Biol. Chem.* **291**, 25815–25822 (2016).
6. B. Chen, S. B. Padrick, L. Henry, M. K. Rosen, *Methods Enzymol.* **540**, 55–72 (2014).
7. T. E. Stradal *et al.*, *Trends Cell Biol.* **14**, 303–311 (2004).
8. B. Chen *et al.*, *eLife* **6**, e29795 (2017).
9. Z. Chen *et al.*, *Nature* **468**, 533–538 (2010).
10. A. M. Lebensohn, M. W. Kirschner, *Mol. Cell* **36**, 512–524 (2009).
11. C. Litschko *et al.*, *Eur. J. Cell Biol.* **96**, 715–727 (2017).
12. L. Shao *et al.*, *Nat. Commun.* **9**, 2377 (2018).
13. S. O. Burns, A. Zarafov, A. J. Thrasher, *Curr. Opin. Hematol.* **24**, 16–22 (2017).
14. M. Kircher *et al.*, *Nat. Genet.* **46**, 310–315 (2014).
15. H. Park *et al.*, *J. Exp. Med.* **205**, 2899–2913 (2008).
16. A. Leithner *et al.*, *Nat. Cell Biol.* **18**, 1253–1259 (2016).
17. C. Basquin *et al.*, *EMBO J.* **34**, 2147–2161 (2015).
18. A. F. Carisey, E. M. Mace, M. B. Saeed, D. M. Davis, J. S. Orange, *Curr. Biol.* **28**, 489–502.e9 (2018).
19. A. Gil-Krzewska *et al.*, *J. Allergy Clin. Immunol.* **142**, 914–927.e6 (2018).
20. S. Murugesan *et al.*, *J. Cell Biol.* **215**, 383–399 (2016).
21. J. C. Nolz *et al.*, *Curr. Biol.* **16**, 24–34 (2006).
22. O. D. Weiner *et al.*, *PLOS Biol.* **4**, e38 (2006).
23. J. C. Nolz *et al.*, *Mol. Cell. Biol.* **27**, 5986–6000 (2007).
24. J. C. Nolz *et al.*, *J. Cell Biol.* **182**, 1231–1244 (2008).
25. D. D. Sarbassov, D. A. Guertin, S. M. Ali, D. M. Sabatini, *Science* **307**, 1098–1101 (2005).
26. A. Diz-Muñoz *et al.*, *PLOS Biol.* **14**, e1002474 (2016).
27. B. Treanor *et al.*, *Immunity* **32**, 187–199 (2010).
28. T. N. Iwata, J. A. Ramírez-Komo, H. Park, B. M. Iritani, *Cytokine Growth Factor Rev.* **35**, 47–62 (2017).
29. C. Yang *et al.*, *eLife* **7**, e35619 (2018).

SUPPLEMENTARY MATERIALS

science.sciencemag.org/content/369/6500/202/suppl/DC1
Materials and Methods
Supplementary Text
Figs. S1 to S12
Tables S1 to S6
References (*30–42*)
Movies S1 to S4

View/request a protocol for this paper from *Bio-protocol*.

Science

HEM1 deficiency disrupts mTORC2 and F-actin control in inherited immunodysregulatory disease

Sarah A. Cook, William A. Comrie, M. Cecilia Poli, Morgan Similuk, Andrew J. Oler, Aiman J. Faruqi, Douglas B. Kuhns, Sheng Yang, Alexander Vargas-Hernández, Alexandre F. Carisey, Benjamin Fournier, D. Eric Anderson, Susan Price, Margery Smelkinson, Wadih Abou Chahla, Lisa R. Forbes, Emily M. Mace, Tram N. Cao, Zeynep H. Coban-Akdemir, Shalini N. Jhangiani, Donna M. Muzny, Richard A. Gibbs, James R. Lupski, Jordan S. Orange, Geoffrey D. E. Cuvelier, Moza Al Hassani, Nawal Al Kaabi, Zain Al Yafei, Soma Jyonouchi, Nikita Raje, Jason W. Caldwell, Yanping Huang, Janis K. Burkhardt, Sylvain Latour, Baoyu Chen, Gehad ElGhazali, V. Koneti Rao, Ivan K. Chinn and Michael J. Lenardo

An inherited disorder makes WAVEs

The WAVE regulatory complex (WRC) is a multiunit complex that regulates actin cytoskeleton formation. Although other actin-regulatory proteins modulate human immune responses, the precise role for the WRC has not yet been established. Cook *et al.* studied five patients from four unrelated families who harbor missense variants of the gene encoding the WRC component HEM1. These patients presented with recurrent infections and poor antibody responses, along with enhanced allergic and autoimmune disorders. HEM1 was found to be required for the regulation of cortical actin and granule release in T cells and also interacted with a key metabolic signaling complex contributing to the disease phenotype. By linking these interactions to immune function, this work suggests potential targets for future immunotherapies.
Science, this issue p. 202

ARTICLE TOOLS	http://science.sciencemag.org/content/369/6500/202
SUPPLEMENTARY MATERIALS	http://science.sciencemag.org/content/suppl/2020/07/08/369.6500.202.DC1
REFERENCES	This article cites 42 articles, 8 of which you can access for free http://science.sciencemag.org/content/369/6500/202#BIBL
PERMISSIONS	http://www.sciencemag.org/help/reprints-and-permissions

Use of this article is subject to the Terms of Service